

Hydrologic flushing rates drive nitrogen cycling and plant invasion in a freshwater coastal wetland model

SEAN J. SHARP ^{1,4}, KENNETH J. ELGERSMA ², JASON P. MARTINA ³, AND WILLIAM S. CURRIE ¹

¹School for Environment and Sustainability, University of Michigan, Ann Arbor, Michigan, 48109 USA

²Department of Biology, University of Northern Iowa, Cedar Falls, Iowa, 50614 USA

³Department of Biology, Texas State University, San Marcos, Texas, 78666 USA

Citation: Sharp, S. J., K. J. Elgersma, J. P. Martina, and W. S. Currie. 2021. Hydrologic flushing rates drive nitrogen cycling and plant invasion in a freshwater coastal wetland model. *Ecology* 31(2):e02233. 10.1002/eap.2233

Abstract. Coastal wetlands intercept significant amounts of nitrogen (N) from watersheds, especially when surrounding land cover is dominated by agriculture and urban development. Through plant uptake, soil immobilization, and denitrification, wetlands can remove excess N from flow-through water sources and mitigate eutrophication of connected aquatic ecosystems. Excess N can also change plant community composition in wetlands, including communities threatened by invasive species. Understanding how variable hydrology and N loading impact wetland N removal and community composition can help attain desired management outcomes, including optimizing N removal and/or preventing invasion by nonnatives. By using a dynamic, process-based ecosystem simulation model, we are able to simulate various levels of hydrology and N loading that would otherwise be difficult to manipulate. We investigate *in silico* the effects of hydroperiod, hydrologic residence time, N loading, and the $\text{NH}_4^+:\text{NO}_3^-$ ratio on both N removal and the invasion success of two nonnative species (*Typha × glauca* or *Phragmites australis*) in temperate freshwater coastal wetlands. We found that, when residence time increased, annual N removal increased up to 10-fold while longer hydroperiods also increased N removal, but only when residence time was >10 d and N loading was >30 g N·m⁻²·yr⁻¹. N removal efficiency also increased with increasing residence time and hydroperiod, but was less affected by N loading. However, longer hydrologic residence time increased vulnerability of wetlands to invasion by both invasive plants at low to medium N loading rates where native communities are typically more resistant to invasion. This suggests a potential trade-off between ecosystem services related to nitrogen removal and wetland invasibility. These results help elucidate complex interactions of community composition, N loading and hydrology on N removal, helping managers to prioritize N removal when N loading is high or controlling plant invasion in more vulnerable wetlands.

Key words: denitrification; ecosystem services; invasive species; nitrogen cycling; nutrient retention; *Phragmites australis*; residence time; *Typha × glauca*; wetland management.

INTRODUCTION

Nutrient loads delivered to lakes and oceans have increased by orders of magnitude in the last half century, often due to changing land use or management practices in their watersheds, such as urban development and agriculture (Howarth et al. 2002). These large nutrient loads can lead to hypoxic dead zones (Diaz and Rosenberg 2008) and harmful algal blooms in receiving waters (Michalak et al. 2013, Lapointe et al. 2015) with consequences that reverberate from aquatic communities to local economies (Hoagland et al. 2002). Wetlands can provide services that mitigate impacts of elevated nutrient loading in some circumstances. For example, constructed wetlands are used as

a tertiary treatment measure to remove large loads of nutrients from effluent (Kadlec and Wallace 1997) while wetlands along the paths of streams and rivers may sequester nutrients from the flow-through water (Knox et al. 2008). This has led many managers to optimize or expand nutrient removal in wetlands within their jurisdiction. However, conditions that improve nutrient removal may hinder other wetland functions and services, such as maintaining plant biodiversity or resisting invasive plant species (Hansson et al. 2005). Understanding the environmental conditions (e.g., water level or nutrient loads) that most influence certain wetland functions can help to optimize the most desired services while minimizing the sacrifice of others (Jessop et al. 2015).

Freshwater wetlands are widespread along lakeshores and in river channels and deltas, and many are hydrologically managed to influence water levels, wildlife habitat, or achieve other goals. In the Laurentian Great Lakes

Manuscript received 17 April 2020; revised 15 July 2020; accepted 16 August 2020. Corresponding Editor: Jason P. Kaye.

⁴E-mail: sjsharp@umich.edu

region of the Upper Midwest, United States, they are also widespread in coastal zones including river mouths and embayments. Because of their position on the landscape, these wetlands receive nutrient loads from surrounding water inflow (both upland runoff and open water fluxes) and can provide important nutrient removal services from these flow-through sources. Specifically, excessive nitrogen (N) loading can be ameliorated through important biotic pathways of removal, including plant uptake (Tylova-Munzarova et al. 2005), immobilization in litter and sediment organic matter (Vymazal 2007), and microbial transformation (e.g., denitrification; Jordan et al. 2015). However, excessive N loading to wetlands may also shift plant community structure, altering ecosystem function and potentially increasing vulnerability of plant communities to invasive species (Erwin 2009, Martina et al. 2016). In turn, the service of wetland N removal is likely to be affected by the interaction among N loading, plant growth and litter production, water levels, and hydrologic residence time (Pezeshki 2001). Given this complex set of interactions, understanding and managing N removal in wetlands is intrinsically challenging, especially when management goals are not complementary (Jessop et al. 2015).

N removal in wetlands is dominated by plant N uptake, immobilization in litter and sediments, and microbial denitrification, which are all controlled by various biotic and abiotic drivers. Removal via plant uptake and immobilization in soil occurs as plants assimilate inorganic N from porewater and overlying water to meet metabolic nutrient demands (Vymazal 2007). However, as plant detritus and soil organic matter decompose, organic N is subject to mineralization and rerelease in place or downstream as detritus and organic matter is flushed out of wetlands (Han et al. 2009). Unlike plant uptake and soil immobilization, denitrification (NO_3^- -N transformation to gaseous N) is a more permanent removal pathway that occurs in anaerobic water and soil and is often coupled with aerobic nitrification, which converts NH_4^+ -N to NO_3^- -N (Reddy et al. 1989). Hydrology, through its control on anaerobic and aerobic conditions, is an important modulator of these N removal mechanisms. For example, hydroperiod determines the phasing and periodicity of aerobic and anaerobic cycles in wetlands that, in turn, control the rate of plant growth and N uptake by controlling soil anoxia (Reed and Cahoon 1992), the rate of litter decomposition, and whether aerobic nitrification or anaerobic denitrification is occurring (Ishida et al. 2006).

N removal is typically greater the more time N spends in wetlands and thus, in addition to hydroperiod, is also controlled by hydrologic residence time (henceforth, RT_h). RT_h modulates the contact time of N with microbes and plant rhizospheres for transformation and uptake, respectively (Kirk and Kronzucker 2005). The relationship of N removal and RT_h has been well studied in flow-through, constructed, and tertiary treatment wetlands (Kadlec and Wallace 1997, Saunders and Kalff

2001, Ishida et al. 2006). Yet N removal in coastal wetlands is rarely studied (but see Dettmann 2007), in part due to the complex hydrology and N transport dynamics of coastal zones. For example, water levels of the Laurentian Great Lakes fluctuate on decadal time scales, changing the hydrologic gradient from upland water sources to the Great Lakes, thus affecting water flow and RT_h of coastal wetlands that intercept these waters (Keough et al. 1999). Variable hydroperiods can further complicate our understanding of N removal in these wetlands. As soils alternate from aerobic to anaerobic with fluctuating water level, obligate aerobic and anaerobic processes change in tandem. The coincidence of fluctuating water levels with seasonal changes in temperature and plant productivity can lead to further complex interactions of N removal drivers. Finally, many N removal studies only focus on abiotic drivers, such as hydrology, and rarely incorporate biotic drivers or peripheral impacts to plant community structure despite well-known feedbacks between biotic and abiotic drivers (Corenblit et al. 2011).

In fact, plant communities have a powerful influence on nutrient cycling and soil biogeochemistry in wetlands, including the accumulation of nutrients stored in detritus (Weltzin et al. 2005). Likewise, greater nutrient availability can shift plant competition dynamics and plant community composition. For example, increased N loading can facilitate invasion of large-stature, nonnative plant species that are better competitors for nutrients and light and deposit more litter than native competitors, thus increasing soil N pools and therefore N removal (Martina et al. 2016, Uddin and Robinson 2017). In particular, the success of *Phragmites australis* and *Typha × glauca*, both noxious, large-stature invaders of Great Lakes and other North American wetlands, is largely driven by increased N loading (Martina et al. 2016). Through superior competition for N and intraspecific N transfers within clones, these invaders can expand to the extent that they create near-monocultures in coastal wetlands (Zedler and Kercher 2004, Rickey and Anderson 2004). In facilitating these invasive plants, N availability likely interacts with other factors including nutrient cycling dynamics and hydrological disturbances (Wilcox 2012, Bansal et al. 2019). To improve our understanding of these complex drivers, we need to examine how hydroperiod and RT_h of coastal wetlands interact to affect N removal and how changes in N removal will potentially alter the invasibility of wetland plant communities (Fig. 1).

Simulation models allow us to explore a wide range of these complex processes and interactions in thousands of structured scenarios and factorial combinations that would be difficult or impossible to perform in field studies. Here we examined in silico how RT_h , hydroperiod, and N loading interact to affect N cycling and N removal rates in emergent wetlands, thereby influencing the outcomes of wetland plant invasions. We examine various hydroperiod frequencies with the same flooding

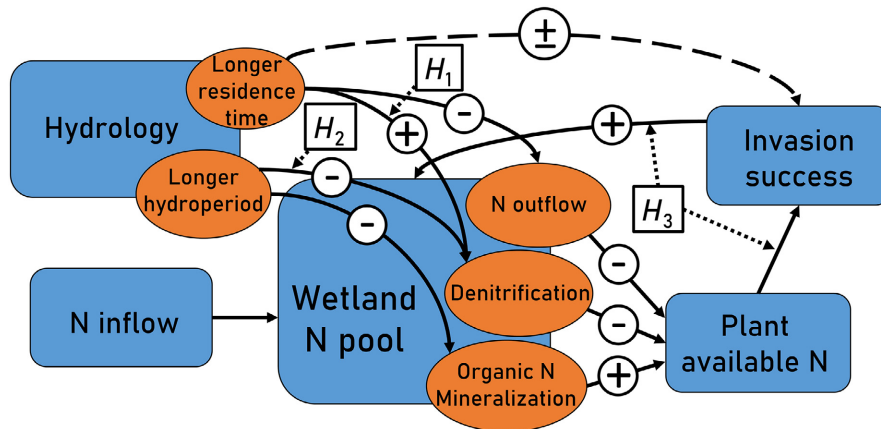


FIG. 1. Conceptual model depicting the influence of various biotic and abiotic drivers on wetland N availability and invasion success of wetland macrophytes. Blue boxes represent larger storages or processes while orange ovals represent smaller processes that occur within the larger blue boxes. Wetland N pool includes inorganic NO_3^- -N and NH_4^+ as well as litter and soil organic N. Solid lines represent direct effects and dashed lines represent indirect effects. H_1 , H_2 , and H_3 boxes represent hypotheses predicting effects of water residence time, hydroperiod, and plant invasions on N cycling.

range and total number of flooded days but with different flooding duration, in addition to wetlands with constant low and high water level. We also examined N loading with various nitrate (NO_3^-) to ammonium (NH_4^+) ratios as N removal and transformation processes can require one or the other species and because these ratios vary across the landscape (Hamlin et al. 2020; L. Wan, *personal communication*). We then assessed how these conditions influence N removal in two ways: annual N removal (i.e., the total N mass removed from an area in a given time) and N removal efficiency (i.e., N removed and denitrified relative to N entering wetlands).

We simulated a range of these hydrologic and nutrient cycling variables in scenarios where one of two nonnative invasive graminoids (*Phragmites australis* or *Typha × glauca*) was introduced into an established native plant community typical of Great Lakes coastal wetlands using Mondrian, a process-based model of wetland ecosystems that includes plant competition and dynamic community change over time. We hypothesized that longer RT_h would increase the percent of N inflow denitrified, while N loading dominated by NH_4^+ would limit denitrification, resulting in less overall N removal (Fig. 1, H_1). Second, we hypothesized that, assuming the total number of flooded days is equal, simulated wetlands with longer hydroperiod would result in less annual denitrification and subsequent N removal (Fig. 1, H_2). When wetlands flood and draw down often, aerobic nitrification, which transforms NH_4^+ to NO_3^- , can also occur more frequently replenishing depleted stocks for denitrifying microbes compared to less frequently flooded wetlands. Finally, in scenarios of long RT_h whereby N inflow exceeds N outflow, we hypothesized that higher levels of plant-available inorganic N would drive the success of wetland plant

invasion and subsequently increase N uptake and ecosystem N removal due to the high N demands of these large-stature invaders (Fig. 1, H_3). We demonstrate the potential for a novel ecosystem trade-off between N removal and invasion risk driven by RT_h in freshwater coastal wetlands.

MATERIALS AND METHODS

Mondrian simulation model

We used an individual-based, spatially explicit wetland ecosystem model, Mondrian, which spans multiple levels of ecological organization from individual plant physiology to population, community, and ecosystem processes. The model was previously developed to study N cycling and plant invasion (Currie et al. 2014, Martina et al. 2016, Elgersma et al. 2017, Goldberg et al. 2017). We give a brief overall description with some detail on processes and functions either newly added or key to understanding the present study.

Mondrian utilizes a grid space that can be divided into ≤ 625 cells. Over this framework of grid cells, a user-defined number of individual propagules (i.e., ramets) are stochastically dispersed. Individual ramets have defined, species-specific traits, including relative growth rate, maximum plant size and tissue nutrient requirements. Ramets within grid cells compete for available N and light within the same cell (for details on light competition, see Martina et al. 2016). Plants clonally reproduce, spreading rhizomes stochastically through the model space, and share resources via translocation among rhizome chains. The modeled substrate is vertically organized with mineral soil organic matter (MSOM) on the bottom, then muck, and aboveground litter on top. Although the thickness of the MSOM layer is fixed

(30 cm), the thicknesses of the muck and litter pools vary depending on relative rates of litter production and decomposition, allowing accretion or subsidence of the muck surface. At the ecosystem level, the user defines daily N inflow, daily water level and water flow rate, daily temperature, and growing season length. Several ecosystem processes emerge from these fine-scale processes, including plant productivity, community composition, and C and N cycling dynamics. The model has balanced C and N cycles and explicitly represents and tracks ecosystem C and N stocks, export, transformation, and removal (defined below).

In this study, we introduce an updated version of Mondrian (version 4.3) parametrized for wetlands of the Great Lakes region with improved realism in certain aspects of clonal plant growth and N cycling. The updated model simulates lateral and terminal branching of rhizomes in clonal plants (see J. P. Martina et al., *unpublished manuscript*, for full description), and now includes flooding-induced mortality for individual plants. It also explicitly partitions available NH_4^+ -N and NO_3^- -N, includes inflow and export of each separately, and includes nitrification and denitrification processes. Finally, the modified model allows flexibility in the inflow and hydrologic flushing rate of N, which can be constant or vary daily.

Nitrification and denitrification

N cycling in Mondrian has been augmented to include coupled nitrification and denitrification, the latter providing an additional N removal pathway. In previous model versions, N that was not taken up by plants or immobilized in detritus was flushed out of the wetland at a certain rate, the balance remaining as plant-available N. We calculate nitrification and denitrification as daily fluxes ($\text{g N}\cdot\text{m}^{-2}\cdot\text{d}^{-1}$) spatially explicit within grid cells, using Eqs. (1) and (2), respectively

$$\begin{aligned} \text{Daily nitrification (gN}\cdot\text{m}^{-2}\cdot\text{day}^{-1}) \\ = I_{\text{amm}} \times f_{\text{aer}}(\text{NH}_4^+) \cdot f(T_{\text{soil}}) \cdot \theta_n \end{aligned} \quad (1)$$

$$\begin{aligned} \text{Daily denitrification (gN}\cdot\text{m}^{-2}\cdot\text{day}^{-1}) \\ = I_{\text{nitr}} \cdot f_{\text{ana}}(\text{NO}_3^-) \cdot F_{\text{resp}} \cdot \theta_d \end{aligned} \quad (2)$$

where, I_{amm} and I_{nitr} represent grid cell NH_4^+ -N and NO_3^- -N pools ($\text{g N}/\text{m}^2$), respectively, and $f(T_{\text{soil}})$ represents the effect of soil temperature. In Mondrian, we assume that for any soil above a defined water level height, soil temperature (T_{soil}) is equal to ambient air temperature and T_{soil} of any flooded soil below this water level equals the temperature of the overlying water. As nitrification requires aerobic conditions and denitrification requires anaerobic, these processes are constrained by the terms $f_{\text{aer}}(\text{NH}_4^+)$ and $f_{\text{ana}}(\text{NO}_3^-)$, which represent the proportion of I_{amm} that is aerobic and I_{nitr} that is anaerobic, respectively. Unlike nitrification, which involves oxidizing ammonia (NH_4^+) to nitrate (NO_3^-) and is modulated by f

(T_{soil}), denitrification is a heterotrophic process and involves the oxidation of labile soil organic C. Heterotrophic respiration, including the effects of temperature and the size of detrital pools, is already included in Mondrian. Therefore, F_{resp} , a unitless factor that tracks rates of soil heterotrophic respiration, conveys a temperature effect and tracks substrate availability for denitrifying microbes in a similar fashion as other denitrification models (Parton et al. 1996). Finally, the model was calibrated to ecosystem-scale observations using scaling parameters for both nitrification (θ_n) and denitrification (θ_d).

Nitrification and denitrification occur in the model within explicit vertical limits we refer to as the “active zone” for each process. This allows us to calculate, based on daily water level, which proportion of the active zone is aerobic and anaerobic. The top of the vertical active zone is defined as the top of the muck layer for denitrification, and for nitrification extends up to 5 cm into the aboveground litter layer above the muck where conditions are likely to be more aerobic than in muck and MSOM, even when flooded. For this study, the lower boundary of the active zone is set to 5 cm depth in the mineral soil, below which the rates for both processes have been observed to be negligible (Brodrick et al. 1988). Any detrital pool (or partial pool) below a 5-d trailing average of water level is anaerobic in the model, but these pools become aerobic when above the water level on a daily basis. Mondrian does not include nitrification or denitrification in the overlying water column. At temperatures below 4°C, rates of nitrification and denitrification are assumed to be negligible (Bremner and Shaw 1958).

To calibrate the ecosystem-level scaling parameters (θ_n and θ_d), we used five sentinel sites from the Great Lakes region with observational data for multiyear data sets of in situ denitrification. We only included studies with field measurements of denitrification (i.e., measured fluxes of $\text{N}_2 + \text{N}_2\text{O}$) and omitted studies that measured only potential denitrification in ideal laboratory settings or with an augmented supply of nitrate. We simulated the relevant conditions reported at each sentinel site in Mondrian, including annual average temperature, temperature range, growing season length, water level, N inputs, and plant community (Table 1). For sites that did not report both NH_4^+ and NO_3^- inputs, we used a 1:3 ratio of NH_4^+ -N: NO_3^- -N, typical of land use dominated by high-intensity agriculture in which these sites were situated (Hamlin et al. 2020). We then adjusted both θ_n and θ_d to achieve a best fit using a residual sum of squares (Fig. 2).

Simulated experimental design

We used five hydroperiods, five RT_b , six levels of N loading, five N species ratios, and two invasion scenarios amounting to 1,380 unique combinations of these

TABLE 1. List of sites, empirical field data, and Mondrian model output and input values used to determine scaling parameters and calibrate denitrification in Mondrian.

Site	Empirical values		Model output		Model input				Source
	Denitrification ($\text{g N}\cdot\text{m}^{-2}\cdot\text{yr}^{-1}$)	Biomass ($\text{g C}/\text{m}^2$)	Denitrification ($\text{g N}\cdot\text{m}^{-2}\cdot\text{yr}^{-1}$)	Biomass ($\text{g C}/\text{m}^2$)	NH_4^+ ($\text{g N}\cdot\text{m}^{-2}\cdot\text{yr}^{-1}$)	NO_3^- ($\text{g N}\cdot\text{m}^{-2}\cdot\text{yr}^{-1}$)	Water depth (cm)	RT_h (d)	
Old Woman Creek, Ohio	10.6	No data	9.3	494	50.2	228	0 ± 100	4.2	McCarthy et al. (2008)
Champaign, Illinois	10.0	500	11.9	494	36.0	144	16 ± 25	7.0	Xue et al. (1999)
St Louis Bay Estuary, Minnesota	5.7	157	0.3	267	0.0	10.8	75 ± 0	13.0	Bellinger et al. (2014)
Olentangy River, Columbus, Ohio	2.7	779	1.2	624	24.5	98.1	-2 ± 40	1.0	Hernandez and Mitsch (2007)
Cheboygan Marsh, Michigan	0.7	591	0.3	281	0.0	12.9	4 ± 6	3.2	Lishawa et al. (2014)

Notes: Mondrian was calibrated using empirical values of annual average denitrification, biomass, nitrogen inputs (NH_4^+ -N and NO_3^- -N), water depth, and hydrologic residence time (RT_h). All locations are in the United States.

factors (Table 2). Here we describe each of these factors in turn. In Mondrian, hydroperiod is controlled by defining water level daily. In these simulations, we used 5 hydroperiods, including permanently flooded (water level +15 cm in relation to the MSOM soil horizon), permanently exposed (water level -15 cm), and sinusoidal fluctuating water level (± 50 cm) with weekly, monthly or semiannual periodicity. These fluctuating hydroperiods reflect weather events that

occur on short (weekly) and medium (monthly) time scales and seasonal (semiannual) fluctuations that occur on a longer time scale with water level peaking in mid-June. All wetlands with variable hydroperiod in these simulations (weekly, monthly, and semiannual) experienced the same maximum flooding depth and total number of days with overlying surface water per year with the only difference being the timing of flooding.

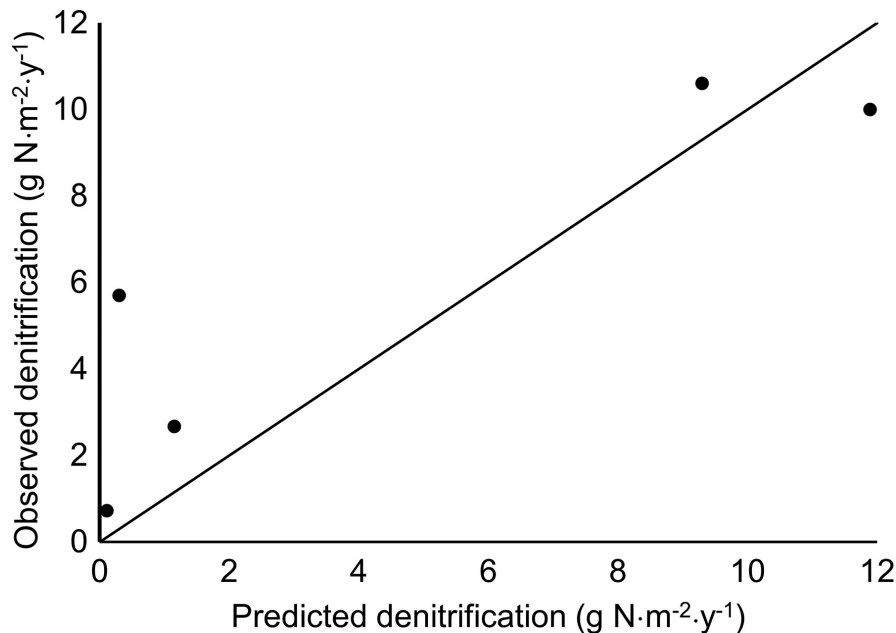


FIG. 2. Observed and simulated values of denitrification from five regional sentinel sites used for Mondrian calibration of ecosystem-level scaling parameters. Diagonal line represents hypothetical 1:1 relationship of predicted model and observed field data.

TABLE 2. Predictor variables and their various factor levels used in model simulations for this study.

N loading (g N·m ⁻² ·yr ⁻¹)	NH ₄ ⁺ -N: NO ₃ ⁻ -N mass ratio	RT _h (d)	Hydroperiod	Plant invader identity
1	0:1	<i>f</i> (water level)	constant 15 cm	<i>Phragmites australis</i>
5	1:7.3	1	constant -15 cm	<i>Phragmites australis</i>
10	1:3	10	weekly (±50 cm)	<i>Typha × glauca</i>
15	4:1	100	monthly (±50 cm)	
30	1:0	365	semiannual (±50 cm)	
100				

Notes: Each predictor variable was crossed in a semi-factorial manner with the other drivers (i.e., RT_h = *f*[water level] was not crossed with constant hydroperiod resulting in *n* = 1,380 unique treatment combinations). RT_h, hydrologic residence time (d).

In Mondrian, the proportion of the NH₄⁺-N and NO₃⁻-N pools exported daily from the wetland is controlled by a hydrologic flushing parameter, which equals the inverse of hydrologic residence time (RT_h). Daily values of RT_h and water level are read in from an input file, allowing simulation of seasonal hydrological trends. For this study, we modeled RT_h either as a fixed rate throughout the simulation (four scenarios independent of water level) or as a function of water level (three scenarios). For fixed rates, we chose RT_h values of 1, 10, 100, and 365 d to capture a range of wetland types found in the Great Lakes region, from a small, flow-through wetland to a coastal embayment with a 1-yr residence time, respectively (Morrice et al. 2004). In our scenario, where RT_h is a function of water level, we used an exponential relationship

$$RT_h = \frac{1}{ae^{bh}} \quad (3)$$

where *a* and *b* are constants, *h* is water level (m), and where lower water level corresponds to longer RT_h. To parameterize the constants *a* and *b*, when water level was lowest, we used RT_h = 365 d and, when water was highest, we used RT_h = 1 d. Under constant water-level scenarios of permanently flooded and permanently exposed, RT_h as a function of water level would also be constant. Therefore, these scenarios are omitted as a treatment combination, leaving only weekly, monthly, and semiannual hydroperiods with RT_h as a function of water level.

In addition to hydroperiod and RT_h, we used six levels of N loading, ranging from oligotrophic, precipitation-fed wetlands (1 g N·m⁻²·yr⁻¹) to highly eutrophic wetlands (100 g N·m⁻²·yr⁻¹; Krieger 2003). We then partitioned the six levels of N loading into NH₄⁺-N and NO₃⁻-N proportions that included conceptual NH₄⁺-only or NO₃⁻-only N inputs as end points, together with three NH₄⁺-N:NO₃⁻-N ratios that characterize wetland N loading from three dominant land use classes in the region: urban (1:7.3), high-intensity agriculture (1:3), and rural (4:1; Hamlin et al. 2020). Finally, we simulated plant communities in which either *Phragmites australis*

or *Typha × glauca*, two common invasive species in the Great Lakes region, are introduced into established communities comprising three native wetland species: *Eleocharis smallii*, *Juncus balticus*, and *Schoenoplectus acutus*. At year 15, after the native community has reached a steady-state density, we introduce a cohort of 15 individual ramets of one of the two invasive species and introduce another identical cohort 5 yr later. A background colonization rate of 1 ramet·yr⁻¹·species⁻¹ continues for all species after initial introduction into the modeling space.

Each of the 1,380 combinations was run for 55 yr, enough time for the simulation to achieve ecosystem stability, with three stochastic replications. Mondrian outputs large amounts of data after each model run ranging from stem density to total ecosystem C. For this study, we averaged all output of the last 5 yr of each simulation (years 51–55) to integrate across inter-annual variation. We limited the response variables we examined to annual N removal (g N·m⁻²·yr⁻¹), percent denitrification (%), N removal efficiency (%), and invader percentage of community net primary productivity, NPP (%). To account for the large disparity between denitrification rates under low and high N loading, we interpreted denitrification as the percentage of annual N inflow denitrified. We define annual N removal (*N*_{rem}) as

$$N_{rem} = N_{in} - N_{out} \quad (4)$$

percent denitrification (*N*_{dnt}) as

$$N_{dnt} = \frac{\text{Annual denitrification (gN} \cdot \text{m}^{-2} \cdot \text{yr}^{-1})}{N_{in} \text{ (gN} \cdot \text{m}^{-2} \cdot \text{yr}^{-1})} \quad (5)$$

and N removal efficiency as

$$\text{N removal efficiency} = \frac{N_{rem}}{N_{in}} \quad (6)$$

where *N*_{in} is the sum of annual N inputs, including annual surface N loading and atmospheric N deposition and *N*_{out} includes the annual hydrologic export of all NO₃⁻-N, NH₄⁺-N, and detritus-bound organic N.

Statistical analysis

We used Generalized Linear Mixed Models (GLMM) to examine the effects of treatment combinations of predictor variables, including N loading, $\text{NH}_4^+\text{-N}:\text{NO}_3^-\text{-N}$ ratio, RT_h , hydroperiod, and plant invader species (Table 2) on total annual N removal, N removal efficiency, percent of annual N inflow denitrified, and invader proportion of community NPP response variables averaged over the last 5 yr of simulations (Bates et al. 2015). N loading and RT_h were analyzed as continuous numeric variables and $\text{NH}_4^+\text{-N}:\text{NO}_3^-\text{-N}$ ratio, hydroperiod, and plant invader species as factors with discrete levels. When RT_h was a function of water level, we used the average annual RT_h ($\text{RT}_h \approx 4$ d) to include this treatment within the range of other continuous RT_h values (see Figs. 3–5). To develop a best-fit GLMM, we used a forward stepwise algorithm in which terms are iteratively added, starting from a null model lower bound to a global model (i.e., a model including all main effects and

their possible interactions) upper bound. This algorithm uses Akaike Information Criterion (AIC) to select the best GLMM by scoring each model based on goodness-of-fit and model parsimony, only adding more terms when such additions improve the AIC value. In addition to ranking models based on AIC and goodness-of-fit (adjusted R^2), we also ranked terms within each best-fit GLMM by their relative variable importance (RVI) value (Burnham and Anderson 2002) to focus our analysis to only the most important main effects and interactions, despite other main effects and interactions also being important, albeit less so (Table 4). RVI values are calculated by summing the Akaike weights, a goodness-of-fit measure of a single model weighted across an array of models, for all possible GLMMs in which a given variable occurs. Because RVI values of main effects and interactions are relative they cannot be directly compared to one another (e.g., RVI values of two-way interaction terms can only be compared to RVI values of other two-way interaction terms and not with RVI values of main effects

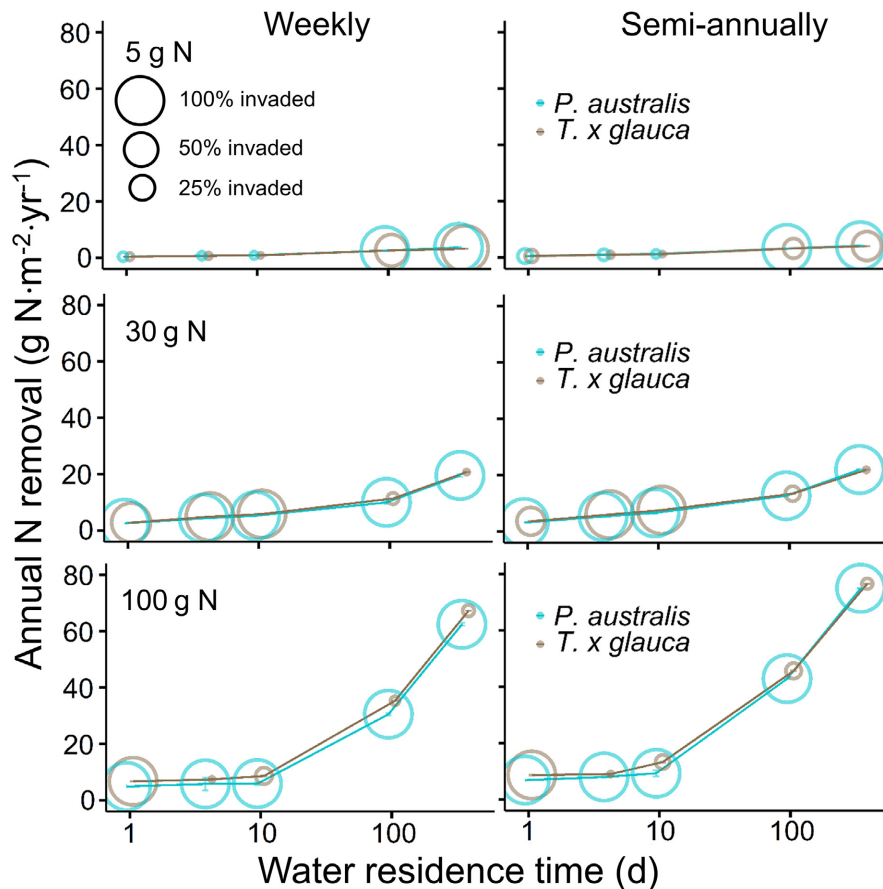


FIG. 3. Annual nitrogen (N) removal as a function of water residence time (RT_h , plotted on a log scale) in simulations of weekly (left panels) and semiannual and permanent (labeled as semiannual; right panels) flooding regimes. Each row of panels corresponds to a different level of wetland N inflow in $\text{g N}\cdot\text{m}^{-2}\cdot\text{yr}^{-1}$. Larger circles represent greater percentage (%) of invader net primary productivity or NPP relative to total community NPP. Points on the x axis that fall between 1 and 10 d represent treatments where residence time was a function of water level with an annual average water residence time of ~ 4 d. Colors represent *Phragmites australis* and *Typha x glauca*. Error bars represent \pm SE of three identical stochastic model runs.

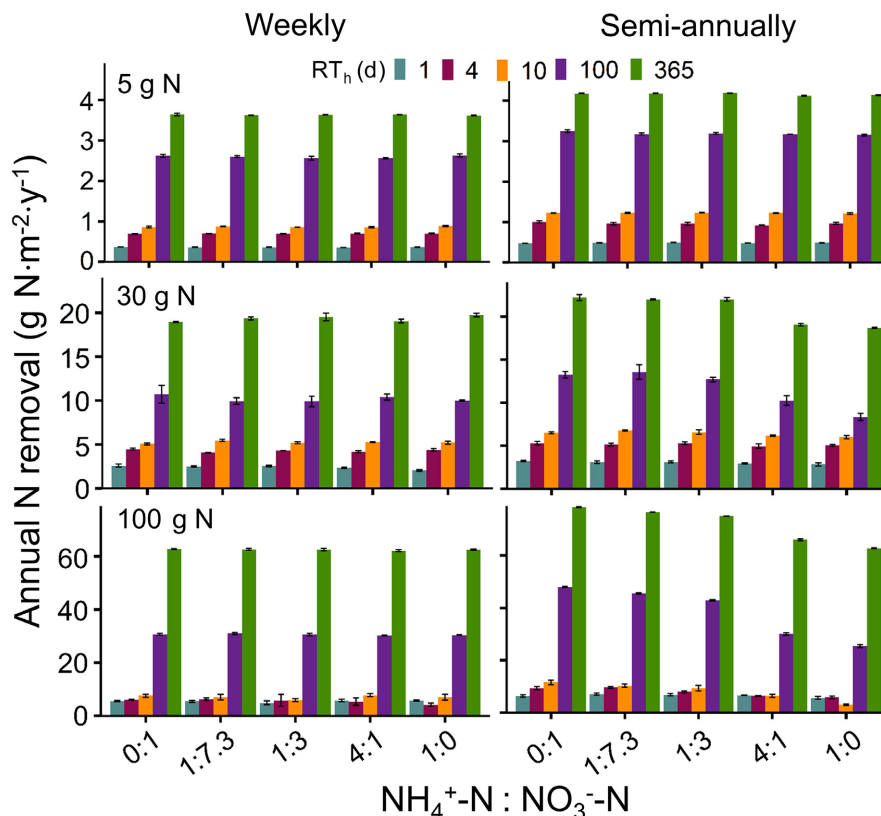


FIG. 4. Annual nitrogen (N) removal across a range of $\text{NH}_4^+\text{-N}:\text{NO}_3^-\text{-N}$ ratios. Ratios of 1:7.3, 1:3, and 4:1 reflect watershed N inputs for urban, high-intensity agriculture, and rural land use classes, respectively. Ratios of 0:1 and 1:0 represent hypothetical ammonium-only and nitrate-only N loading, respectively. Bar colors represent water residence time (RT_h). Error bars represent \pm SE of three identical stochastic model runs.

or higher order interactions), we interpret these terms separately. All data were analyzed using the lme4 (Bates et al. 2015) and MuMIn (Barton 2019) packages in the statistical computing software R version 3.6.1 (R Core Team 2019).

RESULTS

In our simulations of Great Lakes coastal wetlands, we found that hydrologic residence time (RT_h), hydroperiod, and N loading were all strong predictors of wetland N removal, including annual N removal, N removal efficiency, and percent denitrification (Tables 3, 4). Furthermore, these drivers interacted such that N removal was greatest when RT_h and hydroperiod were longest, yet each measure of N removal was affected differently by changes in N loading (Figs. 3–6). Drier wetlands (e.g., wetlands with constant low water) had a limited capacity for N removal compared to flooded wetlands in our simulations. As plant litter and organic matter pools became aerobic, denitrification stopped, decomposition was accelerated, and mineralized N was exported downstream. Alone, $\text{NH}_4^+\text{-N}:\text{NO}_3^-\text{-N}$ ratio and plant invader identity had little influence on any measure of N removal,

but when interacting with N loading were important predictors of annual N removal. Under semipermanent flooding, N removal was greater when N loading had a higher proportion of NO_3^- compared to N loading with a higher proportion of NH_4^+ (Fig. 7). Under high N loading, in communities where *Typha* was introduced but failed to establish, slightly more N was removed annually compared to *Phragmites*-invaded communities. Finally, RT_h , N loading, and to a lesser extent hydroperiod drove N removal and invasion success, while invader identity impacted invasion success but not wetland N removal.

Due to the similarity in outcomes of several treatment levels and in an effort to simplify the presentation of results, we dropped several treatment levels from figures, but still included them in all analyses. We chose a single land-use-derived $\text{NH}_4^+\text{-N}:\text{NO}_3^-\text{-N}$ ratio, 1:3 (representing high-intensity agriculture, the most dominant land cover in the region) because N species ratios had negligible effects in most scenarios. We omitted non-flooded wetlands where N removal was always very low, and combined results from wetlands with permanent and semiannual hydroperiods (hereafter referred to as semi-annual), which always had similar responses to each other. We also omitted the lowest N loading scenario

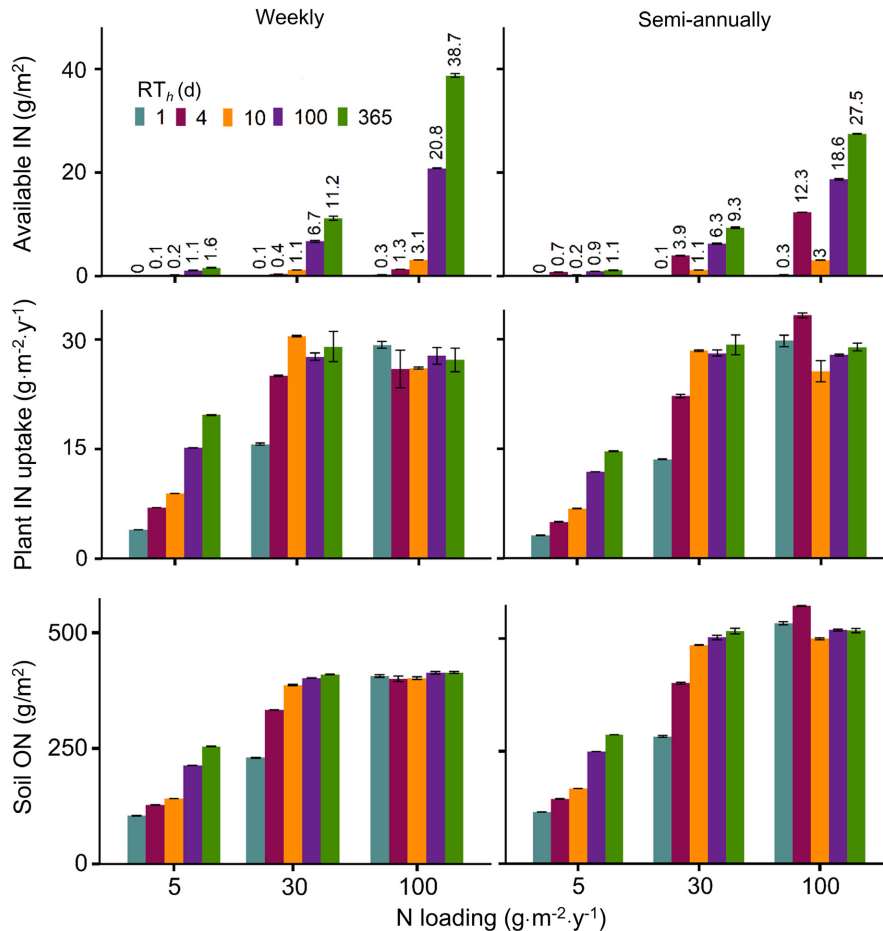


FIG. 5. Plant-available inorganic N (IN; $\text{NH}_4^+\text{-N} + \text{NO}_3^-\text{-N}$), plant IN uptake, and total organic N (ON) in soil pools as a function of N loading in simulations of weekly (left panels) and semiannual and permanent (labeled as semiannual; right panels) flooding regimes. Bar colors represent water residence time (RT_h). Error bars represent \pm SE of three identical stochastic model runs.

($1 \text{ g N}\cdot\text{m}^{-2}\cdot\text{yr}^{-1}$), and only present low ($5 \text{ g N}\cdot\text{m}^{-2}\cdot\text{yr}^{-1}$), medium ($30 \text{ g N}\cdot\text{m}^{-2}\cdot\text{yr}^{-1}$), and high ($100 \text{ g N}\cdot\text{m}^{-2}\cdot\text{yr}^{-1}$) N loading treatments.

Annual N removal

We assessed N removal in either absolute terms of annual N removal ($\text{g N}\cdot\text{m}^{-2}\cdot\text{yr}^{-1}$) or relative terms of N removal efficiency (i.e., N removed and denitrified relative to N entering the wetland). Annual N removal (including soil immobilization, plant uptake, and denitrification; Figs. 3, 5), N removal efficiency (Fig. 6), and percent denitrification (i.e., percentage of N inflow denitrified; Fig. 7) generally increased with longer RT_h , but N loading and RT_h interacted with hydroperiod such that N removal was greatest with longer hydroperiod only under certain combinations of N loading and RT_h . Permanently exposed wetlands exhibiting very low annual N removal as organic N in the soil quickly mineralized (data not shown) and microbes were unable to denitrify under aerobic conditions. Annual N removal (Fig. 3) increased most with

increasing N loading ($5\text{--}100 \text{ g N}\cdot\text{m}^{-2}\cdot\text{yr}^{-1}$) and RT_h ($1\text{--}365 \text{ d}$). However, only under high N loading ($100 \text{ g N}\cdot\text{m}^{-2}\cdot\text{yr}^{-1}$) and $\text{RT}_h > 10 \text{ d}$ did longer hydroperiod (weekly to semiannual) result in a notable increase ($>10 \text{ g N}\cdot\text{m}^{-2}\cdot\text{yr}^{-1}$) in annual N removal. In wetlands with N loading of 30 and $100 \text{ g N}\cdot\text{m}^{-2}\cdot\text{yr}^{-1}$, as RT_h increased from 10 to 100 d annual N removal increased nearly 10-fold while in wetlands with low N loading annual N removal was relatively unaffected by RT_h . In addition to RT_h , hydroperiod, and N loading and their interaction, the interactions of $\text{NH}_4^+\text{-N}:\text{NO}_3^-\text{-N}$ ratios with these main effects were also important predictors of annual N removal (Table 4). Wetlands with semiannual hydroperiod and N loading dominated by NH_4^+ had lower annual N removal compared to wetlands with other N loading ratios because without NO_3^- or the aerobic conditions needed to transform NH_4^+ to NO_3^- in these wetlands, denitrification was arrested (Fig. 4). Invader identity only affected annual N removal under high N loading ($100 \text{ g N}\cdot\text{m}^{-2}\cdot\text{yr}^{-1}$), with native communities where *Typha* was introduced but failed to establish removing approximately

TABLE 3. Values of the differences (Δ) in AIC (Akaike Information Criterion) between each Generalized Linear Mixed Model (GLMM) relative to the best model (in boldface type) of four response variables: annual N removal, percentage of N inflow denitrified, N removal efficiency, and invader percent of total NPP.

Variable and model equation	df	Δ AIC	Adj. R^2
Annual N removal			
$a = \text{N load} \times \text{RT}_h \times \text{Hydro}$	149	355	0.95
$b = a + (\text{N load} \times \text{Hydro} \times \text{N ratio})$	474	37	0.96
$c = b + (\text{N load} \times \text{RT}_h \times \text{N ratio})$	624	13	0.96
$c + (\text{N load} \times \text{RT}_h \times \text{Invader})$	684	0	0.96
N removal efficiency			
$a = (\text{Hydro} \times \text{RT}_h) + (\text{Hydro} \times \text{N load})$	54	97	0.83
$b = a + (\text{N load} \times \text{Invader})$	66	91	0.83
$b + (\text{N load} \times \text{RT}_h \times \text{Hydro})$	161	0	0.84
Percentage of N denitrified			
$a = \text{N load} \times \text{RT}_h \times \text{Hydro}$	149	39	0.83
$b = a + (\text{N ratio} \times \text{N load})$	179	9	0.83
$c = b + (\text{N ratio} \times \text{Hydro})$	209	4	0.83
$c + (\text{N ratio} \times \text{RT}_h)$	234	0	0.83
Invader percentage of total NPP			
$a = \text{N load} \times \text{RT}_h \times \text{Invader}$	59	1	0.31
$a + (\text{RT}_h \times \text{Hydro})$	85	0	0.32

Notes: Model variables include annual N loading (N Load), N species ratio (N ratio), hydrologic residence time (RT_h), hydroperiod (Hydro), and invader species identity (Invader). Included model terms selected base on a forward stepwise selection process. Interaction terms include all lower order interactions and main effects (e.g., three-way interaction includes the three main effects and possible two-way interactions). NPP, net primary productivity. $P < 0.001$ for all models.

5 g N·m⁻²·yr⁻¹ more N than *Phragmites*-invaded communities, a relatively small increase when compared to the differences resulting from longer hydroperiod (>10 g N·m⁻²·yr⁻¹) and longer RT_h (>60 g N·m⁻²·yr⁻¹; Fig. 3). However, at lower rates of N loading, annual N removal was similar across both communities.

The dominant mechanism of N removal in our simulations was uptake by plants and subsequent deposition of plant litter into soil pools, where under anaerobic conditions it accumulates, resulting in the largest N pool in the wetland (soil organic N; Fig. 5). As the major contributor to annual N removal, soil organic N pools similarly increased with longer RT_h , greater N loading, and longer hydroperiod. In particular, soil organic N was limited by aerobic conditions from weekly flooding while semiannually flooded conditions allowed larger soil organic N pools to accumulate. Plant uptake also increased with RT_h and N loading but was not constrained by hydroperiod. Plants and soil pools became somewhat N saturated under N loading of 30 g N·m⁻²·yr⁻¹ when RT_h was ≥ 10 d and across all levels of RT_h under N loading of 100 g N·m⁻²·yr⁻¹ as soil N pools and N uptake plateaued (Fig. 5).

N removal efficiency increased from 6% to 74% under higher N loading as RT_h increased from 1 to

365 d, was slightly higher under longer hydroperiods (Fig. 6). Yet, under low N loading (5 g N·m⁻²·yr⁻¹), N removal efficiency reached only 62% when RT_h was longest. Similar to annual N removal, in semiannually flooded wetlands N removal efficiency was only affected by high NH_4^+ -N: NO_3^- -N ratios in which denitrification was arrested (Appendix S1: Fig. S1). In wetlands with short RT_h (1–10 d), N removal efficiency was consistently low when N loading was high (100 g N·m⁻²·yr⁻¹), unlike wetlands with N loading <100 g N·m⁻²·yr⁻¹ where efficiency steadily increased with increasing RT_h .

Percent denitrification only increased with high N loading (30–100 g N·m⁻²·yr⁻¹) and longer RT_h (100–365 d; Table 3, Fig. 7). In addition, wetlands with semiannual hydroperiod denitrified up to 10 g N·m⁻²·yr⁻¹ more than weekly flooded wetlands and percent denitrification increased from <1% to 69% as RT_h and N loading increased (Fig. 7). The NH_4^+ -N: NO_3^- -N ratio affected denitrification rates only in wetlands with longer, semiannual hydroperiod where obligate aerobic nitrification was inhibited (Appendix S1: Fig. S1). Under semiannual hydroperiod, as N loading became dominated by NH_4^+ -N, denitrification decreased by as much as 89% under high N loading compared to N loading dominated by NO_3^- -N (Appendix S1: Fig. S1) and was negligible (<0.02 g N·m⁻²·y⁻¹) under low N loading.

Community invasion

Invasion was mostly driven by N availability and was even successful under the lowest N loading scenario as longer RT_h resulted in large enough pools of plant-available N to facilitate the dominance of both *Phragmites* and *Typha* over native plant communities (Figs. 4–6; Appendix S1: Fig. S2). Although invader identity was an important predictor of invasion success (measured by percent invader NPP of community NPP), with *Phragmites* a more successful invader than *Typha*, it was not an important predictor of N removal (Table 4). A three-way interaction of invader identity, N loading, and RT_h was also an important predictor of invasion success (Table 3). As RT_h and N loading increased, native communities became increasingly invader dominated, but only up to N loading of 10 g N·m⁻²·yr⁻¹, above which *Phragmites* invasion occurred regardless of RT_h and *Typha* invasion occurred only with shorter RT_h .

Under the lowest N loading regime (1 g N·m⁻²·yr⁻¹), *Phragmites* successfully invaded plant communities (i.e., >75% community NPP) in non-flooded, permanently exposed wetlands with $\text{RT}_h > 100$ d, but failed to establish in any flooded wetlands, regardless of RT_h (Appendix S1: Fig. S2). Yet with each increasing level of N loading and RT_h , *Phragmites* percentage of NPP also increased. At N loading of 30 g N·m⁻²·yr⁻¹, wetlands communities were nearly 100% invaded by *Phragmites* at even the shortest RT_h (1 d). At N loading of

TABLE 4. Relative variable importance (RVI) values of all main effects, two-way, and three-way interactions of predictor variables used in best-fit GLMM models.

Variable	Annual N removal	N removal efficiency	% N denitrified	Invader % of total NPP
Main effect				
RT _h	1.00	1.00	1.00	1.00
Hydro	1.00	1.00	1.00	0.99
N load	1.00	1.00	1.00	1.00
N ratio	0.08	0.21	0.29	0.02
Invader	0.51	0.54	0.66	1.00
Two-way interactions				
RT _h × Hydro	1.00	0.99	0.99	0.65
RT _h × N load	1.00	0.58	0.99	0.99
RT _h × N ratio	0.10	0.03	0.62	0.00
RT _h × Invader	0.36	0.34	0.27	0.99
N load × Hydro	1.00	0.99	0.99	0.26
N load × N ratio	1.00	0.30	0.89	0.00
N load × Invader	1.00	0.90	0.42	0.99
Hydro × N ratio	0.00	0.00	0.08	0.00
Three-way interactions				
N load × RT _h × Hydro	1.00	0.99	0.99	0.00
N load × RT _h × N ratio	1.00	0.00	0.08	0.00
N load × RT _h × Invader	0.99	0.00	0.51	0.72
N load × Hydro × N ratio	1.00	0.91	0.01	0.00

Notes: The highest RVI values within each order (main effect or interactions) of each response variable are shown in boldface type, representing the terms we discuss in this study. Note that RVI is a relative value such that the RVI of main effects and interaction terms can only be compared to similar order terms (e.g., a main effect can be compared to another main effect, but not to any interaction term).

5 g N·m⁻²·yr⁻¹, *Phragmites* invasion was successful at RT_h of 10 d and at 15 g N·m⁻²·yr⁻¹ was successful at RT_h of only 1 d (Appendix S1: Fig. S2).

Typha invasion, however, was successful only in discrete ranges of N loading and RT_h. *Typha* comprised >75% of community NPP at 5–10 g N·m⁻²·yr⁻¹ when RT_h was longest (100 and 365 d) and at 15 g N·m⁻²·yr⁻¹ when RT_h was 4 to 10 d long (Appendix S1: Fig. S2). *Typha* invasion was also successful when N loading was 30–100 g N·m⁻²·yr⁻¹ and RT_h was shorter (1 to 10 days). In scenarios where plant-available N was abundant, yet in which *Typha* did not successfully invade, we observed *Schoenoplectus acutus*, a large-stature native plant, would grow quickly, reaching high NPP similar to a *Typha*-dominated community (~1,750 g C·m⁻²·yr⁻¹). *S. acutus* would fill the model space before year 15 when invaders are introduced in our model, effectively resisting invasion. This mechanism of resistance was confirmed with a set of diagnostic model simulations (Appendix S1: Fig. S3) in which *Typha* was either introduced at year one (rather than year 15), introduced with an equal number of propagules as native species (65 propagules rather than 15), or both (introduced on year 1 with 65 propagules). Only in scenarios in which *Typha* was introduced on year one with 65 propagules did it successfully establish and dominate native communities.

DISCUSSION

Our model findings suggest that while annual N removal increased with both longer RT_h and increasing N loading, N removal efficiency most significantly increased with longer residence time (RT_h). Furthermore, under high N loading, the increase in N removal efficiency with increasing RT_h only occurred in the 100–365 d range. Under low N loading (1–15 g N·m⁻²·yr⁻¹) these same drivers of N removal also facilitated the invasion of *Phragmites australis* and *Typha* × *glauca*. Specifically, we find that longer RT_h can result in an accumulation of N in simulated wetlands that provides more substrate for microbial transformation, like denitrification, and ample nutrients for plants to quickly grow and colonize. This introduces a potential trade-off of ecosystem N removal services and wetland invasion control, whereby hydrologic drivers that facilitate more N removal are also more likely to decrease resistance to invasion by *Phragmites* or *Typha*. Furthermore, these simulations help elucidate complex interactions of hydrology, N loading, and community composition on wetland N removal. As we demonstrate a potential trade-off between N removal and wetland invasibility, we also present practitioners with information to help prioritize management objectives in coastal wetlands that are receiving large amounts of N or are at risk of

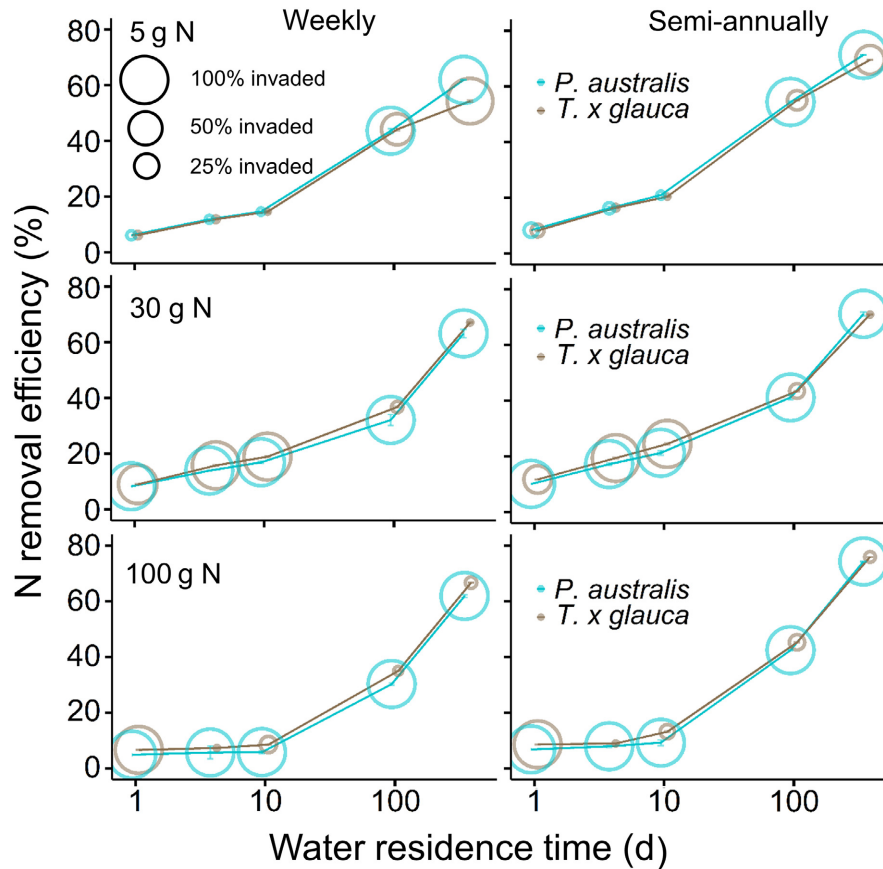


FIG. 6. Nitrogen (N) removal efficiency (N_{rem}/N_{in}) as a function of water residence time (RT_h , plotted on a log scale) in simulations of weekly (left panels) and semiannual and permanent (labeled as semiannual; right panels) flooding regimes. Each row of panels corresponds to a different level of wetland N inflow in $g\ N\ m^{-2}\ yr^{-1}$. Larger circles represent greater percentage (%) of invader net primary productivity (NPP) relative to total community NPP. Points on the x-axis that fall between 1 and 10 d represent treatments where residence time was a function of water level with an annual average water residence time of ~ 4 d. Error bars represent \pm SE of three identical stochastic model runs.

invasion. However, these simulation results should be interpreted cautiously.

Although Mondrian incorporates many complex interactions across several levels of ecological organization, it offers only a functional representation of wetland ecosystems. Mondrian does not include every meaningful mechanism and driver of N removal and invasion in these environments and users should understand the assumptions and limitations of the model before using it as a decision-making tool. For example, in Mondrian the aerobic-anaerobic boundary occurs along a very discrete soil horizon at the top of the water table below the soil surface. In fact, anaerobic conditions and denitrification are known to occur in the overlying water column and be heterogeneous across soil pore space regardless of water table position (Piña-Ochoa and Álvarez-Cobelas 2006, Kjellin et al. 2007). Therefore, Mondrian likely underestimates N removal via denitrification and managers should consider this in their decision-making (Table 1; Fig. 2).

Furthermore, Mondrian does not explicitly model all plant–soil and plant–hydrology interactions, including (but not limited to) gas transport through plant stems, modulation of the rhizosphere environment, plant transpiration, and the drag imposed by vegetation on flowing water. Yet, these mechanisms can be important drivers of N removal processes that should be accounted for when interpreting Mondrian output (Reddy et al. 1989, Chanton and Whiting 1996, Kröger et al. 2009). For example, soil oxygen levels may increase where stem density is high or because of the physiology of particular species, feedbacks which Mondrian does not explicitly model (but that can be accounted for when calibrating the model with empirical data), potentially leading to an underestimation of the proportion of soil that is aerobic. Finally, transpiration and the drag vegetation imposes on flow-through water, important plant–hydrology interactions, are not included in Mondrian but are known to effect water level and RT_h , respectively (Sánchez-Carrillo

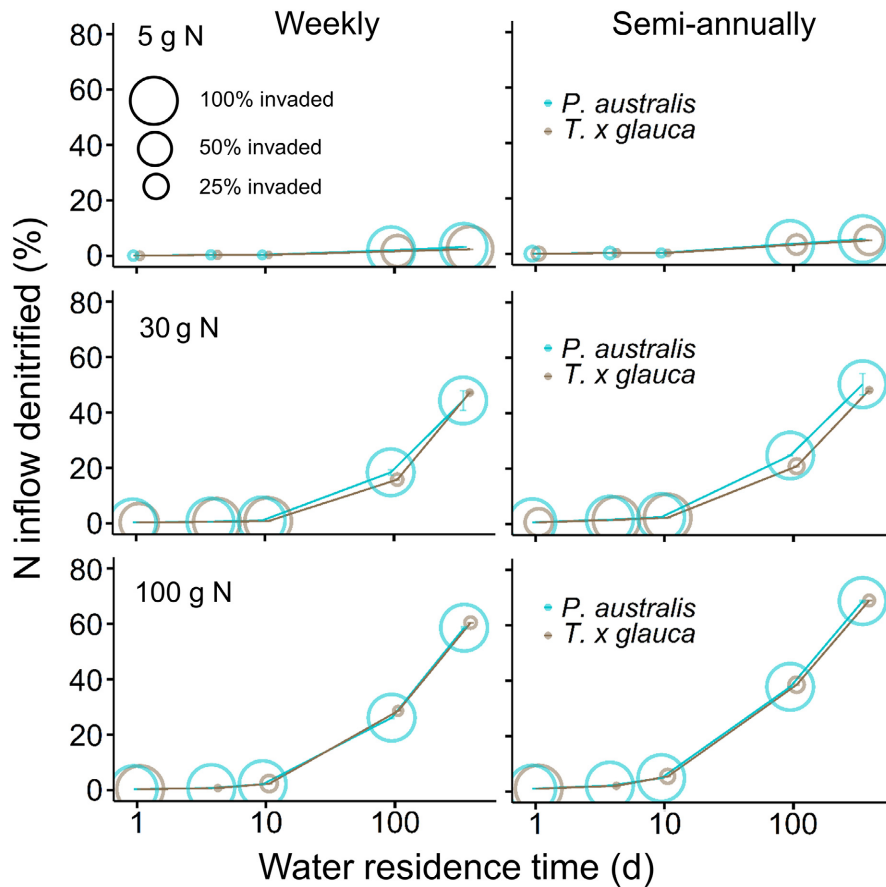


FIG. 7. Percentage (%) of available N from N_{inflow} that is denitrified on an annual basis as a function of water residence time (RT_h , plotted on a log scale) in simulations of weekly (left panels) and semiannual and permanent (labeled as semiannual; right panels) flooding regimes. Each row of panels corresponds to a different level of wetland N inflow in $\text{g N}\cdot\text{m}^{-2}\cdot\text{yr}^{-1}$. Larger circles represent greater percentage (%) of invader net primary productivity (NPP) relative to total community NPP. Points on the x-axis that fall between 1 and 10 d represent treatments where residence time was a function of water level with an annual average water residence time of ~4 d. Error bars represent \pm SE of three identical stochastic model runs. In some instances error bars are smaller than the symbols and are not visible.

et al. 2004, Kröger et al. 2009). However, Mondrian does allow for user-defined, daily changes in water level and RT_h to account for these effects. Despite these limitations, the effect size of RT_h and N loading on N removal and plant invasion is large enough to support use of the general patterns presented in this study to inform wetland management across the region and other freshwater coastal wetlands affected by variable hydrology and N loading.

N removal, RT_h , and denitrification

Inorganic N inputs are initially retained in wetlands through immobilization in microbial communities or assimilation in plants. Annual N removal, which combines plant uptake, soil immobilization, and denitrification, generally increased with more N loading and longer RT_h . Yet, at higher N loading, both annual N removal and N removal efficiency remained low at RT_h

of 1–10 d as soil and plants became N saturated, N was flushed out faster, and there was less N contact time for denitrifying microbes. Surprisingly, under long RT_h (100–365 d), N loading of $100 \text{ g N}\cdot\text{m}^{-2}\cdot\text{yr}^{-1}$ was just as efficient at N removal as wetlands under lower N loading. However, this also indicates that wetlands with high N loading require very long RT_h to be effective at N removal. Supporting our hypothesis and similar to other model analyses (e.g., Dettmann 2007), we found that longer RT_h also increases rates of denitrification. As RT_h increases, the flushing of N out of the system slows, causing it to accumulate in the wetland (Perez et al. 2011). Increases in available N pools supply more N substrate for transformation by denitrifying microbes. Similarly, longer RT_h in the wetland creates more opportunity for plant uptake, thus increasing N removal compared to scenarios with shorter RT_h .

Invader identity had little impact on denitrification in our simulation, despite being recognized as an important

driver in field studies (Findlay et al. 2003). For example, compared to native plants, *Phragmites* provides more labile organic carbon to soil providing energy subsidies for microbes and more oxygen to the rhizosphere, which facilitates nitrification in coupled nitrification–denitrification N removal (Windham and Meyerson 2003, Ehrenfeld 2003). Although Mondrian does include subsidies of organic carbon, it does not explicitly model gas transport in plants and this may result in underestimates of denitrification in our simulations. However, the influence of *Phragmites* in particular can be highly variable (Allred and Baines 2016), and likely driven by small scale variation at spatial resolutions outside the limits of our model. Furthermore, only a small portion of N removal in our studies was attributed to denitrification suggesting the impacts of *Phragmites* on denitrification does not affect the overall patterns of N removal we observed.

Annual N removal was affected by hydroperiod only in extreme scenarios (e.g., non-flooded vs. permanently flooded wetlands). More frequent flooding and shorter hydroperiods did not result in significantly higher percent denitrification as we predicted. Rather, percent denitrification was highest when hydroperiod was longest (e.g., semiannual), although this difference was marginal compared to the large effects incurred by changes in RT_h (Fig. 5). We believe this is due in part to the seasonal timing of flooding in these simulations, a known driver of denitrification and other wetland processes (Valett et al. 2005, Langhans and Tockner 2006). Although wetlands with weekly hydroperiod were flooded the same total number of days in a year as wetlands with semiannual hydroperiod, flooded conditions in semiannual wetlands were concentrated in the growing season (water level peaks during June) when soil temperature is high and microbes are most active. In other words, denitrification conditions were near optimal for all flooded days in semiannual wetlands but only half the flooded days when hydroperiod was weekly, the other flooded days being too cold for denitrification to occur. Only when NO_3^- was scarce (i.e., when $\text{NH}_4^+ \text{-N}:\text{NO}_3^- \text{-N}$ ratios were high) did wetlands with weekly hydroperiod have higher percent denitrification than wetlands with semiannual hydroperiod (Fig. 5). In these scenarios, NO_3^- is limiting and frequent shifts to aerobic soil conditions facilitate oxygen-dependent nitrification, transforming NH_4^+ to NO_3^- needed for denitrification.

Indeed, others have found that under high inputs of NO_3^- , wetlands with longer, less variable hydroperiods removed more N and had higher rates of denitrification than wetlands with more variable, shorter hydroperiods (Ishida et al. 2006). Compared to drier wetlands or wetlands with shorter hydroperiod, wetlands with semiannual hydroperiod remove and store more N as anaerobic conditions slow decomposition of plant litter and mineralization of organic N (Fig. 3). Decomposition and N mineralization are also slowed by low temperatures. Yet

unlike denitrification, N removal via burial of N is less permanent and is more sensitive to changes in oxygen availability and temperature, especially as water levels draw down, or as organic matter is flushed downstream where it may be mineralized later in more oxygen-rich waters (Venterink et al. 2002). Nonetheless, organic N stocks were higher in wetlands with longer hydroperiods, subsidizing overall N removal.

Plant invasion

In addition to increasing N removal, we found that longer RT_h also increases invasion success of *Phragmites australis* and *Typha × glauca*. While it was previously known that there was a threshold of invasion ($\sim 15 \text{ g N}\cdot\text{m}^{-2}\cdot\text{yr}^{-1}$) across a N loading gradient for these two species (Martina et al. 2016), it was unknown that this threshold would be sensitive to RT_h . As RT_h increases, thresholds of successful *Phragmites* invasion shifted towards lower N loads, with invasion occurring even under the lowest N load we simulated ($1 \text{ g N}\cdot\text{m}^{-2}\cdot\text{yr}^{-1}$). When RT_h is longer, N is flushed out of wetlands more slowly and begins to accumulate, resulting in more available N for plant uptake. *Phragmites* is an opportunistic invader capable of outcompeting natives for this available N, growing taller, and shading out neighboring plants (Mozdzer and Zieman 2010, Holdredge and Bertness 2011). Under shorter RT_h , N is quickly flushed from wetlands, reducing available N and preventing rapid *Phragmites* growth and shading of natives (Borin and Tocchetto 2007). However, when N loading exceeded $15 \text{ g N}\cdot\text{m}^{-2}\cdot\text{yr}^{-1}$ even the shortest RT_h we simulated (1 d) cannot prevent *Phragmites* from invading and dominating wetland communities. This suggests that invasion is most sensitive to changes in RT_h in wetlands receiving low inputs of N.

Typha invasion was similarly successful under lower N loading regimes as RT_h lengthened. However, at higher levels of N loading, *Typha* invasion success declined for all RT_h scenarios except the shortest (1 d; Appendix S1: Fig. S2). This outcome is likely due to the robust productivity of natives under high N loads or increased ecosystem N as a result of longer RT_h . As natives grow and reproduce quickly with abundant N in the 15 yr prior to invader introduction, the community is effectively able to prevent *Typha* from invading. We tested this explanation by performing a small set of diagnostic simulations. By increasing *Typha* propagule pressure (65 individuals in a cohort rather than 15) and introducing *Typha* with the native community at year one before the natives can fill the model space, *Typha* was able to dominate the community under high N loading and long RT_h scenarios that it failed to invade if introduced in year 15 (Appendix S1: Fig. S3). This indicates that *Typha* establishment was indeed prevented by the rapid expansion and productivity of the native community, particularly by the larger native, *Schoenoplectus acutus*, which can grow up to 3 m tall (Gleason and Cronquist 1991). This

has been further demonstrated in arid grasslands, where diverse native communities exhibited high resistance to invasion by exotic knapweed, even with abundant available resources thought to facilitate the invader (Maron and Marler 2007). We believe this response was unique to *Typha*, and not observed in *Phragmites* invasion scenarios, because of their differences in physiology and morphology. Compared to *Typha*, *Phragmites* has a higher relative growth rate, maximum size, and leaf architecture that more completely shades neighboring plants, allowing it to outcompete even the densest stand of natives (Martina et al. 2016).

CONCLUSIONS

Reducing nutrient loads downstream and controlling invasive species are both common management objectives and we found that optimizing one may come at the cost of the other. Optimizing management to mitigate negative outcomes is practical in wetlands where hydrology and RT_h can be directly controlled, like tertiary treatment wetlands or waterfowl impoundments (Winton et al. 2016). The simulations we present are modeled after coastal wetlands of the Great Lakes, where controlling hydrology is more difficult and occurs less often (Wilcox 1993). Process-based simulation models, like Mondrian, provide needed insight into functions governed by complex interactions of drivers, including hydrology and nutrient loading, which would be difficult to infer from field studies. In Great Lakes wetlands, RT_h is modulated by multiyear water level fluctuations that determine the direction and rate of water flow in river mouths and along coastlines. With accurate predictions of lake levels, practitioners can anticipate changes in RT_h and subsequent shifts in N removal services and wetland invasibility. For example, when lake levels are high, the hydrologic gradient from coastal wetlands to the lake is shallower, wetland water outflow is slower, and RT_h is longer. In these scenarios, management strategies should focus on invasion threats as longer that results from high lake level will facilitate greater N removal, reducing the need for intervention. When lake levels are lower, priorities should shift to reducing N loading into wetlands, when ideal conditions for N removal decline as downslope hydrologic gradients increase, RT_h shortens, and invasion resistance increases, particularly wetlands receiving $\leq 15 \text{ g N}\cdot\text{m}^{-2}\cdot\text{yr}^{-1}$ where changes in RT_h can be a determining factor of wetland invasibility.

These results can provide timely guidance in the management of both N delivery to the Great Lakes and invasion of vulnerable coastal wetlands as Great Lakes watersheds continue to deliver high amounts of N (Choquette et al. 2019) and lakes experience record-breaking water levels (Gronewold and Rood 2019). By combining lake level predictions with our understanding of invasive species propagation and land use change impacts on watershed nutrient transport we can prioritize

intervention in wetlands most vulnerable to change while optimizing those with high potential for service provisioning. Although our results are specific to Great Lakes coastal wetlands, these trends and trade-offs are general enough to be applied to other freshwater coastal wetlands with similar seasonal hydrology and climate. Furthermore, Mondrian's ability to simulate complex mechanisms shared among temperate herbaceous wetlands throughout time and across regions gives practitioners freedom to explore scenario-specific management strategies by simply defining the environmental setting (e.g., climate patterns, hydrology, and plant communities). This control allows users to fine-tune model predictions to seasonal timing of N delivery, anticipated shifts in seasonal hydrology patterns, including timing of high water, and climate change impacts on wetland biota to further enhance our understanding of the future and function of important and vulnerable coastal wetlands.

ACKNOWLEDGMENTS

We thank Anthony Kendall, Sherry Martin, and Luwen Wan at Michigan State University Hydrogeology Lab for providing analysis of instream nutrient data. Funding for this work was provided by NASA IDS Grant #80NSSC17K0262.

LITERATURE CITED

- Aldred, M., and S. B. Baines. 2016. Effects of wetland plants on denitrification rates: a meta-analysis. *Ecological Applications* 26:676–685.
- Bansal, S., et al. 2019. *Typha* (Cattail) invasion in North American wetlands: Biology, regional problems, impacts, ecosystem services, and management. *Wetlands* 39:645–684.
- Barton, K. 2019. MuMIn: Multi-Model Inference. R package version 1.43.15. <http://r-forge.r-project.org/projects/mumin>
- Bates, D., M. Martin, B. Bolker, and S. Walker. 2015. Fitting linear-effects models using lme4. *Journal of Statistical Software* 67:1–48.
- Bellinger, B. J., T. M. Jicha, L. P. Lehto, L. R. Seifert-Monson, D. W. Bolgrien, M. A. Starry, T. R. Angradi, M. S. Pearson, C. Elonen, and B. H. Hill. 2014. Sediment nitrification and denitrification in a Lake Superior estuary. *Journal of Great Lakes Research* 40:392–403.
- Borin, M., and D. Tocchetto. 2007. Five year water and nitrogen balance for a constructed surface flow wetland treating agricultural drainage waters. *Science of the Total Environment* 380:38–47.
- Bremner, J. M., and K. Shaw. 1958. Denitrification in soil. II. Factors affecting denitrification. *Journal of Agricultural Science* 51:40–52.
- Brodrick, S. J., P. Cullen, and W. Maher. 1988. Denitrification in a natural wetland receiving secondary treated effluent. *Water Research* 22:431–439.
- Burnham, K. P., and D. R. Anderson. 2002. Model selection and multimodel inference: a practical information-theoretic approach. Second edition. Springer, New York, New York, USA.
- Chanton, J. P., and G. J. Whiting. 1996. Methane stable isotopic distributions as indicators of gas transport mechanisms in emergent aquatic plants. *Aquatic Botany* 54:227–236.
- Choquette, A. F., R. M. Hirsch, J. C. Murphy, L. T. Johnson, and R. B. Confesor. 2019. Tracking changes in nutrient

- delivery to western Lake Erie: approaches to compensate for variability and trends in streamflow. *Journal of Great Lakes Research* 45:21–39.
- Corenblit, D., A. C. W. Baas, G. Bornette, J. Darrozes, S. Delmotte, R. A. Francis, A. M. Gurnell, F. Julien, R. J. Naiman, and J. Steiger. 2011. Feedbacks between geomorphology and biota controlling Earth surface processes and landforms: A review of foundation concepts and current understandings. *Earth-Science Reviews* 106:307–331.
- Currie, W. S., D. E. Goldberg, J. Martina, R. Wildova, E. Farner, and K. J. Elgersma. 2014. Emergence of nutrient-cycling feedbacks related to plant size and invasion success in a wetland community-ecosystem model. *Ecological Modelling* 282:69–82.
- Dettmann, E. H. 2007. Effect of water residence time on annual export and denitrification of nitrogen in estuaries: A model analysis. *Estuaries* 24:481.
- Diaz, R. J., and R. Rosenberg. 2008. Spreading dead zones and consequences for marine ecosystems. *Science* 321:926–929.
- Ehrenfeld, J. G. 2003. Effects of exotic plant invasions on soil nutrient cycling processes. *Ecosystems* 6:503–523.
- Elgersma, K. J., J. P. Martina, D. E. Goldberg, and W. S. Currie. 2017. Effectiveness of cattail (*Typha* spp.) management techniques depends on exogenous nitrogen inputs. *Elementa: Science of the Anthropocene* 5:19.
- Erwin, K. L. 2009. Wetlands and global climate change: the role of wetland restoration in a changing world. *Wetlands Ecology and Management* 17:71–84.
- Findlay, S., P. Groffman, and S. Dye. 2003. Effects of *Phragmites australis* removal on marsh nutrient cycling. *Wetlands Ecology and Management* 11:157–165.
- Gleason, H. A., and A. Cronquist. 1991. *Manual of vascular plants of northeastern United States and adjacent Canada*, 2nd edition. New York Botanical Garden, The Bronx, New York, USA. 910 p.
- Goldberg, D. E., J. P. Martina, K. J. Elgersma, and W. S. Currie. 2017. Plant size and competitive dynamics along nutrient gradients. *American Naturalist* 190:229–243.
- Gronewold, A. D., and R. B. Rood. 2019. Recent water level changes across Earth's largest lake system and implications for future variability. *Journal of Great Lakes Research* 45:1–3.
- Hamlin, Q. F., A. D. Kendall, S. L. Martin, H. D. Whitenack, J. A. Roush, B. A. Hannah, and D. W. Hyndman. 2020. Quantifying landscape nutrient inputs with spatially explicit nutrient source estimate maps. *Journal of Geophysical Research Biogeosciences* 125:1–24.
- Han, H., J. D. Allan, and D. Scavia. 2009. Influence of climate and human activities on the relationship between watershed nitrogen input and river export. *Environmental Science and Technology* 43:1916–1922.
- Hansson, L., C. Bronmark, P. Anders Nilsson, and K. Abjornsson. 2005. Conflicting demands on wetland ecosystem services: nutrient retention, biodiversity or both? *Freshwater Biology* 50:705–714.
- Hernandez, M. E., and W. J. Mitsch. 2007. Denitrification in created riverine wetlands: Influence of hydrology and season. *Ecological Engineering* 30:78–88.
- Hoagland, P., D. M. Anderson, Y. Kaoru, and A. W. White. 2002. The economic effects of harmful algal blooms in the United States: Estimates, assessment issues, and information needs. *Estuaries* 25:819–837.
- Holdredge, C., and M. D. Bertness. 2011. Litter legacy increases the competitive advantage of invasive *Phragmites australis* in New England wetlands. *Biological Invasions* 13:423–433.
- Howarth, R. W., A. Sharpley, and D. Walker. 2002. Sources of nutrient pollution to coastal waters in the United States: Implications for achieving coastal water quality goals. *Estuaries* 25:656–676.
- Ishida, C. K., J. J. Kelly, and K. A. Gray. 2006. Effects of variable hydroperiods and water level fluctuations on denitrification capacity, nitrate removal, and benthic-microbial community structure in constructed wetlands. *Ecological Engineering* 28:363–373.
- Jessop, J., G. Spyreas, G. E. Pociask, T. J. Benson, M. P. Ward, A. D. Kent, and J. W. Matthews. 2015. Tradeoffs among ecosystem services in restored wetlands. *Biological Conservation* 191:341–348.
- Jordan, S. J., J. Stoffer, J. A. Nestlerode, and J. A. Nestlerode. 2015. Wetlands as sinks for reactive nitrogen at continental and global scales: A meta-analysis. *Ecosystems* 14:144–155.
- Kadlec, R. H., and S. Wallace. 1997. *Treatment wetlands*. Page journal of environmental quality. CRC Press, Boca Raton, Florida, USA.
- Keough, J. R., T. A. Thompson, G. R. Guntenspergen, and D. A. Wilcox. 1999. Hydrogeomorphic factors and ecosystem responses in coastal wetlands of the Great Lakes. *Wetlands* 19:821–834.
- Kirk, G. J. D., and H. J. Kronzucker. 2005. The potential for nitrification and nitrate uptake in the rhizosphere of wetland plants: a modelling study. *Annals of Botany* 96:639–646.
- Kjellin, J., S. Hallin, and A. Wörmán. 2007. Spatial variations in denitrification activity in wetland sediments explained by hydrology and denitrifying community structure. *Water Research* 41:4710–4720.
- Knox, A. K., R. A. Dahlgren, K. W. Tate, and E. R. Atwill. 2008. Efficacy of natural wetlands to retain nutrient, sediment and microbial pollutants. *Journal of Environment Quality* 37:1837.
- Krieger, K. A. 2003. Effectiveness of a coastal wetland in reducing pollution of a Laurentian Great Lake: hydrology, sediment, and nutrients. *Wetlands* 23:778–791.
- Kröger, R., M. T. Moore, M. A. Locke, R. W. Steinriede, R. F. Cullum, C. T. Bryant, S. Testa, and C. M. Cooper. 2009. Evaluating the influence of wetland vegetation on chemical residence time in Mississippi Delta drainage ditches. *Agricultural Water Management* 96:1175–1179.
- Langhans, S. D., and K. Tockner. 2006. The role of timing, duration, and frequency of inundation in controlling leaf litter decomposition in a riverfloodplain ecosystem (Tagliamento, northeastern Italy). *Oecologia* 147:501–509.
- Lapointe, B. E., L. W. Herren, D. D. Debortoli, and M. A. Vogel. 2015. Evidence of sewage-driven eutrophication and harmful algal blooms in Florida's Indian River Lagoon. *Harmful Algae* 43:82–102.
- Lishawa, S. C., K. J. Jankowski, P. Geddes, D. J. Larkin, A. M. Monks, and N. C. Tuchman. 2014. Denitrification in a Laurentian Great Lakes coastal wetland invaded by hybrid cattail (*Typha × glauca*). *Aquatic Sciences* 76:483–495.
- Maron, J., and M. Marler. 2007. Native plant diversity resists invasion at both low and high resource levels. *Ecology* 88:2651–2661.
- Martina, J. P., W. S. Currie, D. E. Goldberg, and K. J. Elgersma. 2016. Nitrogen loading leads to increased carbon accretion in both invaded and uninvaded coastal wetlands. *Ecosphere* 7:1–19.
- McCarthy, M. J., W. S. Gardner, P. J. Lavrentyev, K. M. Moats, F. J. Jochem, and D. M. Klarer. 2008. Effects of hydrological flow regime on sediment-water interface and water column nitrogen dynamics in a Great Lakes coastal wetland (Old Woman Creek, Lake Erie). *Journal of Great Lakes Research* 33:219–231.
- Michalak, A. M., et al. 2013. Record-setting algal bloom in Lake Erie caused by agricultural and meteorological trends

- consistent with expected future conditions. *Proceedings of the National Academy of Sciences USA* 110:6448–6452.
- Morrice, J. A., J. R. Kelly, A. S. Trebitz, A. M. Cotter, and M. L. Knuth. 2004. Temporal dynamics of nutrients (N and P) and hydrology in a Lake Superior coastal wetland. *Journal of Great Lakes Research* 30:82–96.
- Mozdzer, T. J., and J. C. Zieman. 2010. Ecophysiological differences between genetic lineages facilitate the invasion of non-native in North American Atlantic coast wetlands. *Journal of Ecology* 98:451–458.
- Parton, W. J., A. R. Mosier, D. S. Ojima, D. W. Valentine, D. S. Schime, K. Weier, and A. E. Kulmala. 1996. Generalized model for N₂ and N₂O production from nitrification and denitrification. *Global Biogeochemical Cycles* 10:401–412.
- Perez, B. C., J. W. Day, D. Justic, R. R. Lane, and R. R. Twilley. 2011. Nutrient stoichiometry, freshwater residence time, and nutrient retention in a river-dominated estuary in the Mississippi delta. *Hydrobiologia* 658:41–54.
- Pezeshki, S. R. 2001. Wetland plant responses to soil flooding. *Environmental and Experimental Botany* 46:299–312.
- Piña-Ochoa, E., and M. Álvarez-Cobelas. 2006. Denitrification in aquatic environments: A cross-system analysis. *Biogeochemistry* 81:111–130.
- R Core Team 2019. R: A language and environment for statistical computing. R Foundation for Statistical Computing, Vienna, Austria.
- Reddy, K. R., W. H. Patrick, and C. W. Lindau. 1989. Nitrification-denitrification at the plant root-sediment interface in wetlands. *Limnology and Oceanography* 34:1004–1013.
- Reed, D., and D. Cahoon. 1992. The relationship between marsh surface topography, hydroperiod, and growth of *Spartina alterniflora* in a deteriorating Louisiana salt marsh. *Journal of Coastal Research* 8:77–87.
- Rickey, M. A., and R. C. Anderson. 2004. Effects of nitrogen addition on the invasive grass *Phragmites australis* and a native competitor *Spartina pectinata*. *Journal of Applied Ecology* 41:888–896.
- Sánchez-Carrillo, S., D. G. Angeler, R. Sánchez-Andrés, M. Álvarez-Cobelas, and J. Garatuzza-Payán. 2004. Evapotranspiration in semi-arid wetlands: Relationships between inundation and the macrophyte-cover:open-water ratio. *Advances in Water Resources* 27:643–655.
- Saunders, D. L., and J. Kalff. 2001. Nitrogen retention in wetlands, lakes and rivers. *Hydrobiologia* 443:205–212.
- Sharp, S. 2020. Hydrologic flushing rates drive nitrogen cycling and plant invasion in a freshwater coastal wetland model Ecological Applications EAP20-0253 Reproducible Data Archive. Data set. University of Michigan - Deep Blue. <https://doi.org/10.7302/thef-4p55>
- Tylova-Munzarova, E., B. Lorenzen, H. Brix, and O. Votrubova. 2005. The effects of and on growth, resource allocation and nitrogen uptake kinetics of *Phragmites australis* and *Glyceria maxima*. *Aquatic Botany* 81:326–342.
- Uddin, M. N., and R. W. Robinson. 2017. Responses of plant species diversity and soil physical-chemical-microbial properties to *Phragmites australis* invasion along a density gradient. *Scientific Reports* 7:11007.
- Valett, H. M., M. A. Baker, J. A. Morrice, C. S. Crawford, M. C. Molles, C. N. Dahm, D. L. Moyer, J. R. Thibault, and L. M. Ellis. 2005. Biogeochemical and metabolic responses to the flood pulse in a semiarid floodplain. *Ecology* 86:220–234.
- Venterink, H. O., T. E. Davidsson, K. Kiehl, and L. Leonardson. 2002. Impact of drying and re-wetting on N, P, and K dynamics in a wetland soil. *Plant and Soil* 243:119–130.
- Vymazal, J. 2007. Removal of nutrients in various types of constructed wetlands. *Science of the Total Environment* 380:48–65.
- Weltzin, J. F., J. K. Keller, S. D. Bridgman, J. Pastor, P. B. Allen, and J. Chen. 2005. Litter controls plant community composition in a northern fen. *Oikos* 110:537–546.
- Wilcox, D. A. 1993. Effects of water level regulation on wetlands of the Great Lakes. Environmental Science and Ecology Faculty Publications, Brockport, New York, USA. 90 p.
- Wilcox, D. A. 2012. Response of wetland vegetation to the post-1986 decrease in Lake St. Clair water levels: Seed-bank emergence and beginnings of the *Phragmites australis* invasion. *Journal of Great Lakes Research* 38:270–277.
- Windham, L., and L. A. Meyerson. 2003. Effects of common reed (*Phragmites australis*) expansions on nitrogen dynamics of tidal marshes of the northeastern U.S. *Estuaries* 26:452–464.
- Winton, R. S., M. Moorman, and C. J. Richardson. 2016. Waterfowl impoundments as sources of nitrogen pollution. *Water, Air, & Soil Pollution* 227:1–13.
- Xue, Y., D. A. Kovacic, M. B. David, L. E. Gentry, R. L. Mulvaney, and C. W. Lindau. 1999. In situ measurements of denitrification in constructed wetlands. *Journal of Environment Quality* 28:263.
- Zedler, J. B., and S. Kercher. 2004. Causes and consequences of invasive plants in wetlands: Opportunities, opportunists, and outcomes. *Critical Reviews in Plant Sciences* 23:431–452.

SUPPORTING INFORMATION

Additional supporting information may be found online at: <http://onlinelibrary.wiley.com/doi/10.1002/eap.2233/full>

DATA AVAILABILITY

Data are available from the Deep Blue repository at the University of Michigan (Sharp 2020): <https://doi.org/10.7302/thef-4p55>.